Progress In Electromagnetics Research C, Vol. 79, 185–198, 2017

A Novel Reconfigurable UWB Filtering-Antenna with Dual Sharp Band Notches Using Double Split Ring Resonators

Ammar Alhegazi*, Zahriladha Zakaria, Noor Azwan Shairi, Imran Mohd Ibrahim, and Sharif Ahmed

Abstract—This study presents a novel technique for designing an ultra-wideband (UWB) filtering-antenna with dual sharp band notches. This design is composed of a modified monopole antenna integrated with resonant structures. The monopole antenna is modified using microstrip transition between the feedline and the patch. In addition, block with a triangle-shaped slot is loaded on each side of the ordinary circular patch to produce wide bandwidth with better return loss and higher frequency skirt selectivity. The resonant structures are constructed using two double split ring resonators (DSRR) loaded above the ground plane of the antenna to produce dual band notches and filter out WiMAX (3.3–3.7 GHz) and HiperLAN2 (5.4–5.7 GHz) frequencies. The band notch position is controlled by varying the length of the DSRR. The reconfigurability feature is achieved by using two PIN diode switches employed in the two DSRR. The measured results show that the proposed filtering-antenna provides wide impedance bandwidth from 2.58 to 15.5 GHz with controllable dual sharp band notches for WiMAX and HiperLAN, peak realized gain of 4.96 dB and omnidirectional radiation pattern.

1. INTRODUCTION

Ultra-wideband (UWB) is a communication method used in wireless technology for transmitting large amounts of data over short distance with very low energy level over a large portion of the radio spectrum. The main feature of the UWB technology is the ability to carry signals through doors and other obstacles that tend to reflect signals with high power and limited bandwidth, thus it has been incorporated with other fields such as wireless communications, radar and medical engineering [1–3]. Antenna is a main element in the UWB system to transmit and receive signals. Most researchers tend to use monopole antennas to achieve UWB response due to their attractive features such as easy manufacture, low cost, omnidirectional radiation high data rate and wide frequency bandwidth which is suitable for UWB applications [4]. However, UWB technology is facing interference problem with other narrowband systems such as WiMAX (3.3–3.7 GHz), HiperLAN2 (5.47–5.725 GHz) and WLAN (5.15–5.35 GHz, 5.725–5.825 GHz) [5–7]. Thus, a microwave bandstop filter is integrated into the UWB system to remove unwanted signals and reduce the possible interference. The conventional UWB system is integrated with the filter in a separated module from the antenna which leads to increasing the size, cost and losses [8], Therefore, it is desirable to integrate the microwave filter and antenna into a single design to provide radiating and filtering functions simultaneously. Recently, reconfigurability applications are used in modern technology [9]. Thus reconfigurable antennas have gained tremendous research interest in many applications such as cellular radio system, radar applications [10], aircraft, mobile, satellite communications, Unmanned Airborne Vehicle (UAV) radar, smart weapon protection

Received 23 September 2017, Accepted 10 November 2017, Scheduled 24 November 2017

* Corresponding author: Ammar Alhegazi (ammarhejazy@hotmail.com).

The authors are with the Centre of Telecommunication Research and Innovation (CeTRI), Fakulti Kejuruteraan Elektronik dan Kejuruteraan Komputer (FKEKK), Universiti Teknikal Malaysia Melaka (UTeM), Hang Tuah Jaya, Durian Tunggal 76100, Melaka, Malaysia .

and microwave imaging that requires flexibility to support many standards (e.g., UMTS, Bluetooth, WiFi, WiMAX, DSRC), mitigate strong interference signals and cope with the changing environmental condition [11, 12].

The antenna with filtering function is known as filtering-antenna or filtenna. Filtering-antenna has several advantages such as miniaturized size, low cost, and reduced losses [13]. Thus, there is growing interest to integrate resonant structures in the antenna to achieve filtering function using different techniques. Some researchers produced the band rejection by introducing resonant structures in the radiation patch of the antenna [14–21]. Three U-slots were defected on a fractal patch to produce dual band notches have been applied in [22]. Some others used defected ground structure (DGS) [23, 24]. Another technique is using resonator structures beside the feedline of the antenna [25]. Incorporating active components into the resonant structure to achieve frequency reconfiguration was studied in [26–28]. However, the disadvantage of these techniques is excessive band rejection, thus, most of these antennas reject whole WLAN frequencies (5.15–5.35 GHz, 5.725–5.825 GHz) including HiperLAN2 frequencies (5.47–5.725 GHz), Therefore, producing sufficient and sharp band notches is a challenging issue.

In this study, a modified monopole antenna is designed to achieve wide impedance bandwidth. To reduce the possible interference in the UWB system and provide dual sharp band notches, two DSRR are loaded above the ground plane of the antenna. Therefore, the proposed design has sharper band notches than recently published dual band notches UWB antennas in Table 1. The position of the band notch is controlled by varying the length of the DSRR. By employing a PIN diode switch in each DSRR, the reconfigurability feature is achieved.

2. ANTENNA DESIGN

The antenna is designed and simulated using Computer Simulation Technology (CST). The substrate material used for this design is Rogers RT/Duroid 5880, which has a relative permittivity of $\varepsilon_r = 2.2$, loss tangent of $\tan\delta = 0.0009$ and thickness of $d = 0.787\,\text{mm}$. The radius (r) of the circular disc monopole antenna and the width (w) of the microstrip feedline are calculated by [29–31]:

$$r = \frac{c\chi'}{2\pi f_o\sqrt{\varepsilon_r}} \tag{1}$$

$$\frac{w}{h} = \frac{\pi}{2}\left[\begin{array}{l} B - 1 - \ln(2B-1) + \dfrac{\varepsilon_r - 1}{2\varepsilon_r}\times \\ \left\{\ln(B-1) + 0.39 - \dfrac{0.61}{\varepsilon_r}\right\} \end{array}\right] \tag{2}$$

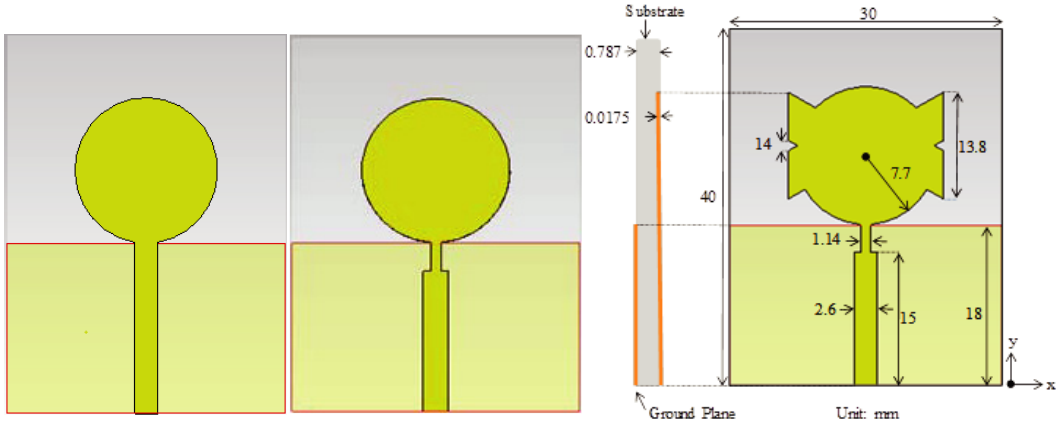

Figure 1. Simulated structures for: (a) Ordinary circular monopole antenna, (b) Antenna with feedline modification and (c) Antenna with feedline and patch modifications.

Table 1. Comparison of recently published dual band notches UWB antennas with the proposed design.

Reference	Band Notch Technique	Bandwidth (GHz)	Band Notches			
			f_{o1} (GHz)	BW1 (MHz)	f_{o2} (GHz)	BW2 (MHz)
[15]	Elliptical ring slot and S-shaped slits etched into the patch	2.6–23	5.55	900	3.5	800
[16]	E-shaped and L-shaped slits etched in the radiating patch	2.89–17.83	5.525	850	3.885	830
[17]	Split ring resonator defected inside the patch	2.9–12	5.96	400	4.04	480
[18]	T-shaped stub and two sets of compound band notched structures in the front layer of the design	3.1–10.6	5.5	700	3.5	600
[19]	U-shaped slot etched on a rectangular patch and a circular ring parasitizes the patch	3.04–17.30	5.475	750	3.75	900
[20]	T-shaped strip and a pair of L-shaped slots located in the radiating patch	2.5–10.8	5.45	1000	3.7	1070
[21]	W-shaped conductor backed-plane structure and a modified T-shaped slot in the radiating patch and microstrip feedline	2.73–13.3	5.495	950	3.95	460
[22]	Three U-slots defected on a monopole fractal patch	3.1–10.6	5.535	990	3.69	780
[23]	Rectangular-slot in the ground structure and a C-shaped slot in the patch	3.1–10.6	5.9	1000	3.9	1200
[24]	Modified G-shaped slot defected in the ground plane and two Γ-shaped stubs located in the patch	2.8–11.8	5.55	900	3.55	500
[25]	Two C-shaped stubs beside the feedline and spiral shaped slot defected in the feedline	2.4–11.6	5.65	1100	3.55	900
[26]	An inverted Γ-shaped parasitic element placed inside the patch and a rectangular split ring resonator placed on the back side	3.1–13	5.4	600	7.5	600
[27]	two open-ended L-shaped slots (OEL-S) and one U-shaped slot Defected Ground Structure	2.7–12	5.5	800	3.45	500
[28]	Two U-shaped slots with folded arm on radiating patch	2.78–12.8	5.46	1040	3.54	580
Proposed	Two DSRR located above the ground plane	2.58–15.68	5.7	300	3.67	460

$$B = \frac{377\pi}{2Z_0\sqrt{\varepsilon_r}} \tag{3}$$

where, $\chi' = 1.8412$, c is the velocity of light and f_o the center frequency.

Regarding the modifications of the ordinary circular monopole antenna shown in Figure 1(a), by introducing a simple microstrip transition between the feedline and the printed circular disc as shown in Figure 1(b), the impedance bandwidth of the planar monopole can be extended as explained in detail in [32]. Loading a block with triangular shape slot on both sides of the ordinary circular patch as shown in Figure 1(c) provides wider impedance bandwidth than the antennas shown in Figures 1(a) and 1(b). Figure 2 shows the simulated return loss of the antennas shown in Figure 1. The results show that the ordinary circular monopole antenna obtains a frequency bandwidth from 3.27 to more than 16 GHz with average return loss above −15 dB, thus by introducing simple microstrip transitions between the feedline and the printed circular disc, the return loss is improved with a good frequency skirt selectivity covering the frequency band from 3.17 to 13.0 GHz. In addition, by loading a block with a triangular shape slot on both sides of the ordinary circular patch, the return loss at higher frequencies is improved. The antenna with feedline and patch modifications shows that a high frequency skirt selectivity covers the frequency band from 3.0 to 14.0 GHz covering the UWB frequency band (3.1–10.6 GHz). Table 2 shows a comparison between the antennas in Figure 1. It can be seen that the antenna in Figure 1(c) has the widest bandwidth and highest gain.

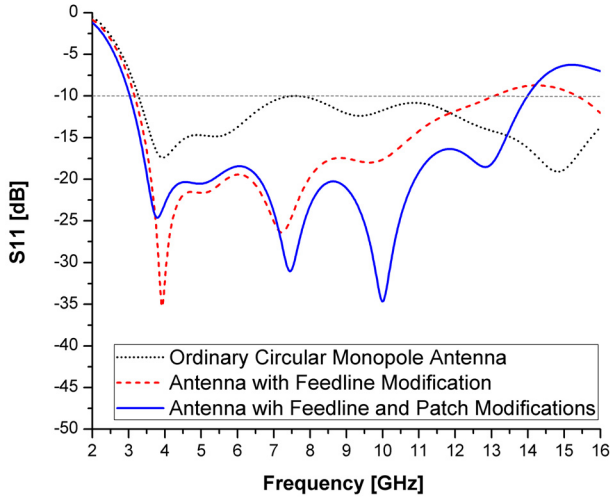

Figure 2. Simulated return loss of the antennas shown in Figure 1.

Table 2. Comparison between antennas in Figure 1.

Structure	Bandwidth (GHz)	Peak Realized Gain (dB)
a	3.27 to more than 16	4.6
b	3.17–13.0	4.45
c	3.0–14.0	5.3

3. FILTERING-ANTENNA DESIGN

To reduce the possible interference with other narrow-band signals such as WiMAX and HiperLAN2, and produce notch characteristics, the UWB antenna is integrated with a resonant structure. The resonant structure is constructed using a split ring resonator (SRR) placed above the ground plane as shown in Figure 3(a). However, the return loss of the band notch using SRR is below −5 dB, thus to improve the return loss of the band notch, the SRR is modified to DSRR as shown in Figure 3(b). To create another band notch, another DSRR with different dimensions is placed above the first DSRR as shown in Figure 3(c), where the first DSRR filters out the HiperLAN2 frequencies, and the second

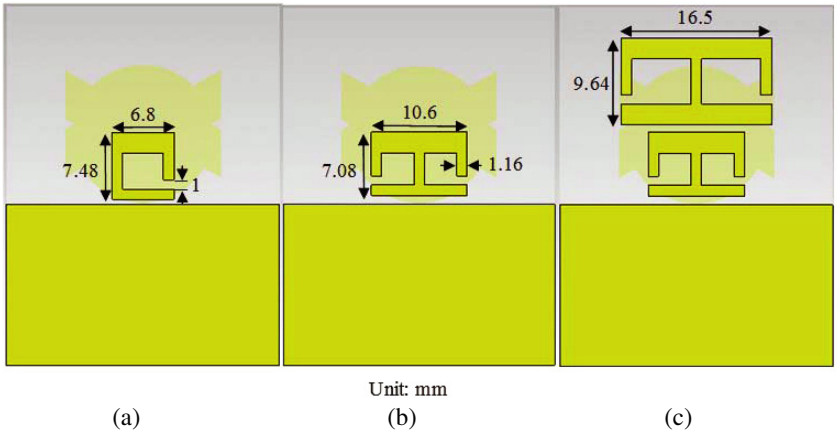

Figure 3. Simulated structures of the proposed antenna with: (a) Single split ring resonator (SRR). (b) Double split ring resonator (DSRR) and (c) Two double split ring resonators (DSRR).

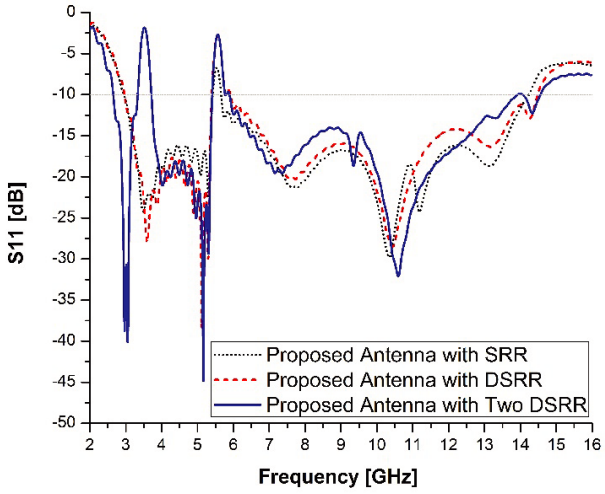

Figure 4. Simulated return loss of the antennas shown in Figure 3.

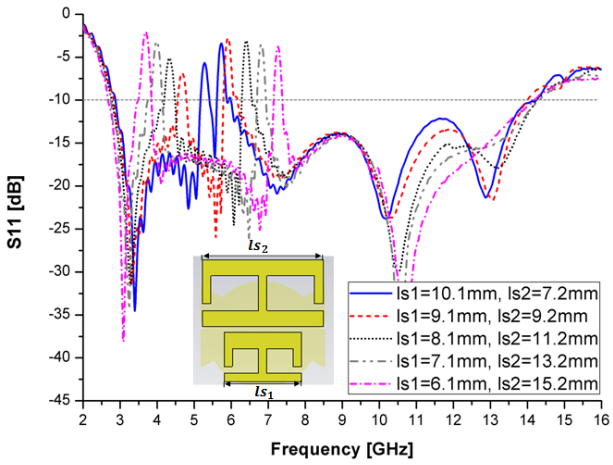

Figure 5. Simulated return loss of the proposed antenna with length variation of the DSRR.

DSRR filters out the WiMAX frequencies. Figure 4 shows the simulated return loss of the antennas shown in Figure 3.

The lengths of the resonant structures are approximately quarter wavelength of the frequencies around 3.5 GHz and 5.55 GHz. In addition, the position of the created band notch is controlled by changing the length of the DSRR as shown in Figure 5. It can be observed that as the length of the resonant structure increases the resonant frequency decreases and vice versa. Furthermore, the new integration using DSRR can filter out upper and lower WLAN frequency bands (5.15–5.35 GHz and 5.7–5.8 GHz) at the same time where $ls_1 = 10.1$ mm and $ls_2 = 7.2$ mm, whereas most recently published dual band notches UWB antennas in Table 1 tended to reject whole WLAN frequencies (5.15–5.35 GHz, 5.725–5.825 GHz) including HiperLAN2 frequencies (5.47–5.725 GHz).

Figure 6 shows the surface current distribution at the band notches frequencies. It can be seen that the current is more concentrated on the DSRR and flows in opposite directions with the same amounts which cancel each other and leads to high attenuation, thus the antenna does not radiate, and therefore band notch is created [24].

The two DSRR above the ground plane can be modeled by RLC equivalent circuit, where each DSRR acts as a parallel RLC circuit as shown in Figure 7. The parallel capacitance, inductance, and

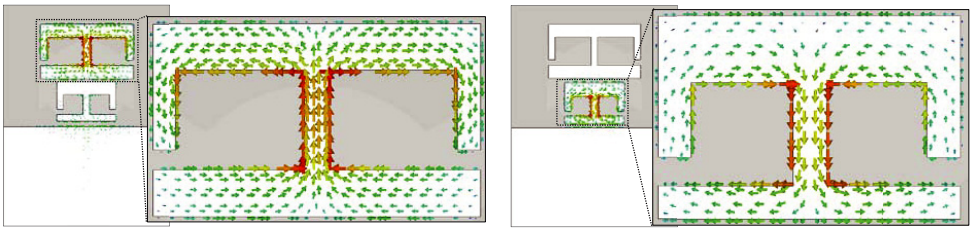

Figure 6. Simulated surface current distribution at (a) 3.5 GHz and (b) 5.55 GHz.

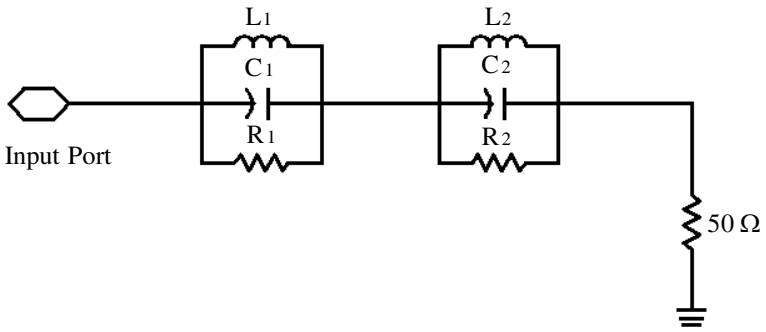

Figure 7. Equivalent circuit model of the two DSRR above the ground plane of the antenna.

resistance are calculated by using the following equations [33, 34]:

$$C = \frac{f_c}{200\pi\left(f_o^2 - f_c^2\right)} \tag{4}$$

$$L = \frac{1}{4\pi^2 f_o^2 C} \tag{5}$$

$$Q_o = \frac{f_o}{BW} \tag{6}$$

$$R = \frac{Q_o}{2\pi f_o C} \tag{7}$$

where, f_o and f_c are the centre and cutoff frequencies, respectively. Q_o and BW are the loaded quality factor and 3 dB notch bandwidth, respectively. Based on the equations given above, the values of the lumped elements in Figure 7 are calculated and listed in Table 3. The first and second RLC circuits are calculated at resonant frequencies of 5.55 GHz and 3.5 GHz, respectively.

Table 3. Calculated values of the lumped elements in Figure 7.

RLC Circuit	BW (MHz)	Q_o	R (Ω)	L (nH)	C (pF)
1	120	46.3	254	0.16	5.23
2	146	24	283	0.54	3.86

4. RECONFIGURABILITY CONFIGURATION

An ideal switch (SW) is inserted in each DSRR to achieve frequency reconfiguration as shown in Figure 8(a). The ideal switch is about copper strip, where the presence of the copper strip shows

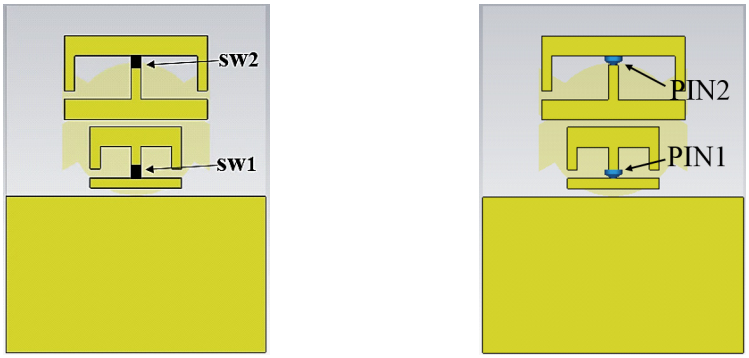

Figure 8. Simulated structure of the proposed design using (a) Ideal switches and (b) PIN diode switches.

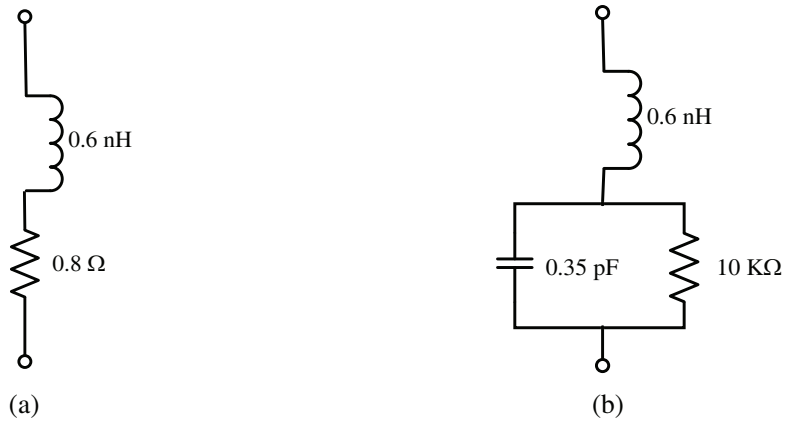

Figure 9. RLC equivalent circuit of the BAP64-02 PIN diode at (a) ON and (b) OFF states.

that the DSRR acts as a short circuit (SC) and represents the ON state, while the absence of the copper strip shows that the DSRR acts as an open circuit (OC) and represents the OFF state [35].

Figure 8(b) shows the proposed filtering-antenna with PIN diode switches. The PIN diode switches are used to achieve frequency reconfiguration, which acts as a variable resistor with two operating statuses (ON/OFF) [36]. The operating modes of the PIN diode can be modelled by an RLC circuit which consists of low resistance that allows the current to pass through the PIN diode and acts as a short circuit in the ON state, while in the OFF state, it consists of parallel capacitance and large resistance that block the flow of the current through the PIN diode and acts as open circuit. Figure 9 shows the equivalent RLC circuit of the BAP64-02 with required values [37].

5. RESULTS AND DISCUSSIONS

Figure 10 shows the simulated results of the proposed design using ideal switches. The results show that the proposed design has four operating cases as illustrated in Table 4. When all switches are in ON status, the antenna in case 1 provides wide bandwidth (< -10 dB) from 2.65 to 14.56 GHz with dual band notches (> -10 dB) at 5.57 GHz and 3.52 GHz. In case 2, when SW1 is in ON status and SW2 in OFF state, the antenna operates at wide bandwidth (< -10 dB) from 2.65 to 14.56 GHz with single band notch (> -10 dB) at 5.57 GHz, while in case 3, when SW2 is in ON status and SW1 in OFF state, the antenna has the same bandwidth with single band notch (> -10 dB) at 3.52 GHz. When all switches are in OFF status, the antenna in case 4 provides wide bandwidth (< -10 dB) from 2.65 to 14.56 GHz without band notches.

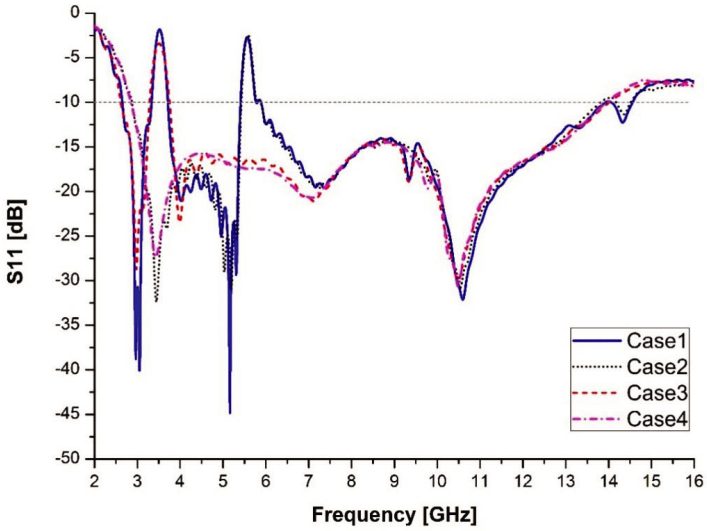

Figure 10. Simulated return loss of the proposed design with four operating cases using ideal switches.

Table 4. Simulated operating cases of the proposed design using ideal switches.

Case	SW1	SW2	Notch (GHz)
1	ON	ON	5.55, 3.5
2	ON	OFF	5.55
3	OFF	ON	3.5
4	OFF	OFF	None (UWB antenna)

Figure 11 shows the fabricated structure of the proposed design. Figure 12 shows the simulated and measured return losses of the proposed design in case 1 and case 4 using ideal switches. The results show that the proposed antenna in case 1 has a wideband performance which covers the UWB frequency band (3.1–10.6 GHz) with sufficient and sharp dual band notches for WiMAX and HiperLAN2 bands, where the simulated result in case 1, when all switches are in ON status, shows a frequency bandwidth ranging from 2.65 to 14.56 GHz with dual band notches at 3.3 to 3.7 GHz and 5.4 to 5.77 GHz, while the result in case 4, when all switches are in OFF status, shows the same frequency bandwidth without band notches. On the other hand, the measured result in case 1, when all switches are in ON status, shows a frequency bandwidth ranging from 2.58 to 15.68 GHz with dual band notches at 3.44 to 3.9 GHz and 5.55 to 5.85 GHz, while the result in case 4, when all switches are in OFF status, shows almost the same frequency bandwidth without band notches. Therefore, it can be said that the simulated and measured results are in a good agreement. However, small frequency shift is noted which is mainly due to the fabrication tolerances and loss tangent of the substrate which expresses the variation in the permittivity of the substrate (2.2 ± 0.02) [38]. The variation in the permittivity of the substrate leads to frequency shift as shown in Figure 13. Table 5 shows a comparison between the simulated and measured results of the proposed design in cases 1 and 4 using ideal switches.

Figure 14 shows the simulated and measured results of the proposed design using PIN diode switches. The results show that the proposed design has four operating cases as illustrated in Table 6. The simulated results show that when all PIN diodes are in ON status, the antenna in case 1 provides wide bandwidth from 2.64 to 14.56 GHz with dual band notches at 5.3 GHz and 3.4 GHz. In case 2, when PIN1 is in ON status and PIN2 in OFF state, the antenna operates at wide bandwidth from 2.64 to 14.56 GHz with single band notch at 5.3 GHz, while in case 3, when PIN2 is in ON status and PIN1 in OFF state, the antenna has the same bandwidth with single band notch at 3.4 GHz. When all PIN diodes are in OFF status, the antenna in case 4 provides wide bandwidth from 2.64 to 14.56 GHz

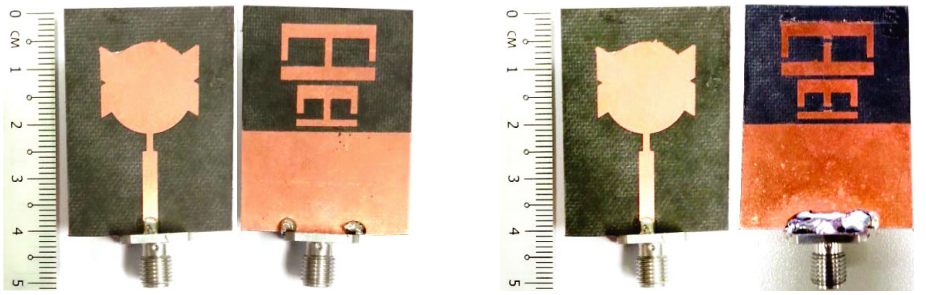

Figure 11. Fabricated filtering-antenna using ideal switches at (a) Case 1, and (b) Case 4.

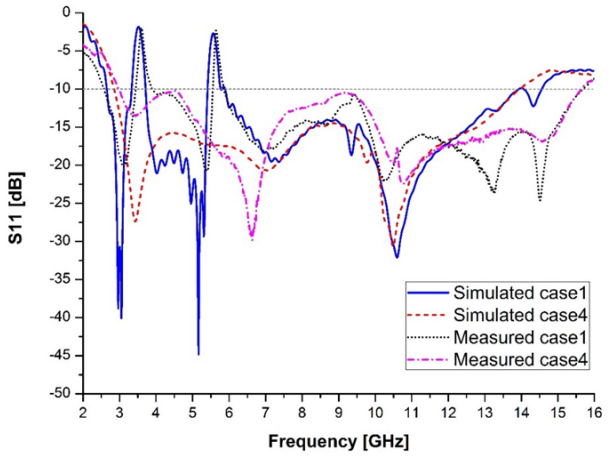

Figure 12. Simulated and measured return loss of the proposed design in case 1 and 4 using ideal switches.

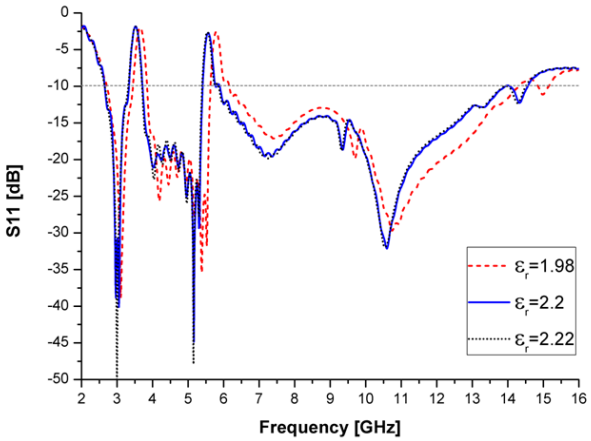

Figure 13. Simulated return loss of the proposed design with permittivity variation of the substrate.

Table 5. Simulated and measured operating cases of the proposed design using ideal switches.

Case	SW1	SW2	Band Notches (GHz)	
			Simulated	Measured
1	ON	ON	5.57, 3.52	5.7, 3.67
4	OFF	OFF	None (UWB antenna)	None (UWB antenna)

without band notches. However, comparing Tables 5 and 6, it can be observed that the simulated band notches are shifted from 5.57 and 3.52 to 5.3 and 3.4, respectively, due to the influence of the inductance of the PIN diode at the ON state. Therefore, tune the band notches back by changing the length of the two DSRR. The measured results show that when all PIN diodes are in ON status, the antenna in case 1 provides wide bandwidth from 2.58 to 15.5 GHz with dual band notches at 5.1 GHz and 3.36 GHz. In case 2, when PIN1 is in ON status and PIN2 in OFF status, the antenna operates at wide bandwidth from 2.58 to 15.5 GHz with single band notch at 5.1 GHz, while in case 3, when PIN2 is in ON status and PIN1 in OFF status, the antenna has the same bandwidth with single band notch at 3.36 GHz. When all PIN diodes are in OFF status, the antenna is in case 4 provides wide impedance bandwidth from 2.58 to 15.5 GHz without band notches. However, a frequency shift is noted between the simulated and

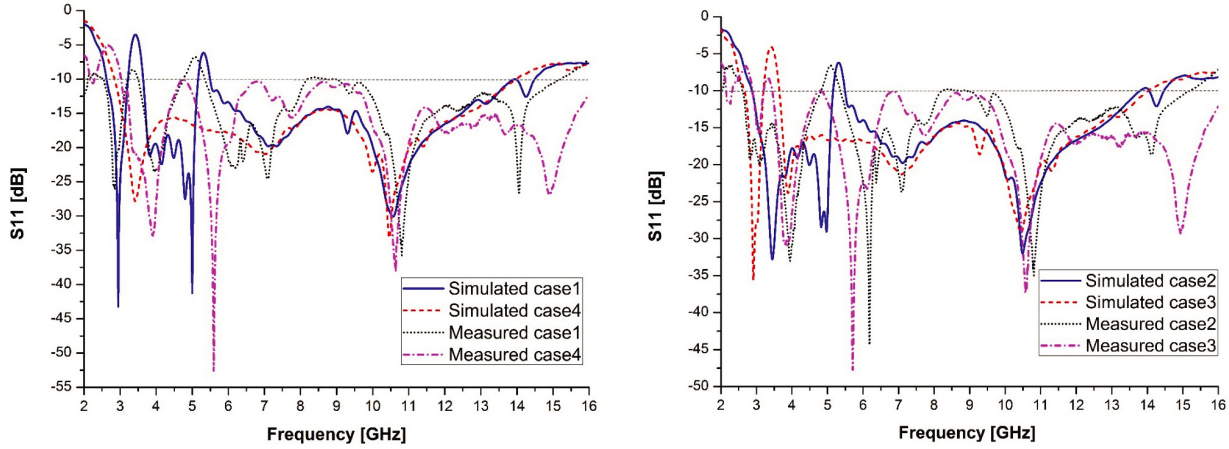

Figure 14. Simulated and measured results of the proposed design at (a) Case 1 and 4, and (b) Case 2 and 3 using PIN diode switches.

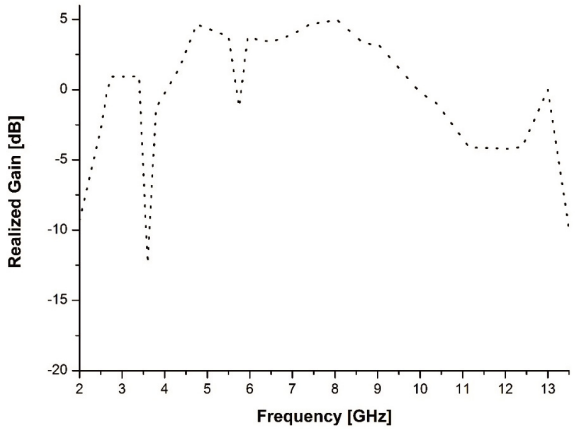

Figure 15. Measured realized gain of the proposed filtering-antenna in case 1 using ideal switches.

Table 6. Simulated and measured operating cases of the proposed design using PIN diode switches.

Case	PIN1	PIN2	Notch (GHz)	
			Simulated	Measured
1	ON	ON	5.3, 3.4	5.1, 3.36
2	ON	OFF	5.3	5.1
3	OFF	ON	3.4	3.36
4	OFF	OFF	None (UWB antenna)	None (UWB antenna)

measured results where the band notches at 3.4 GHz and 5.3 GHz are shifted to 3.36 GHz and 5.1 GHz, respectively. It is believed that this is due to loss tangent of substrate, fabrication tolerances and biasing network. It can also be due to the difference between the behavior of the actual PIN diode and the modeled PIN diode which leads to frequency shift [39]. In addition, the return loss of the measured band notches decreases compared to the simulated one which is mainly due to the current limit of the PIN diode at the ON state, where the maximum supplied voltage is 1.1 Volt [40]. Moreover, the performance

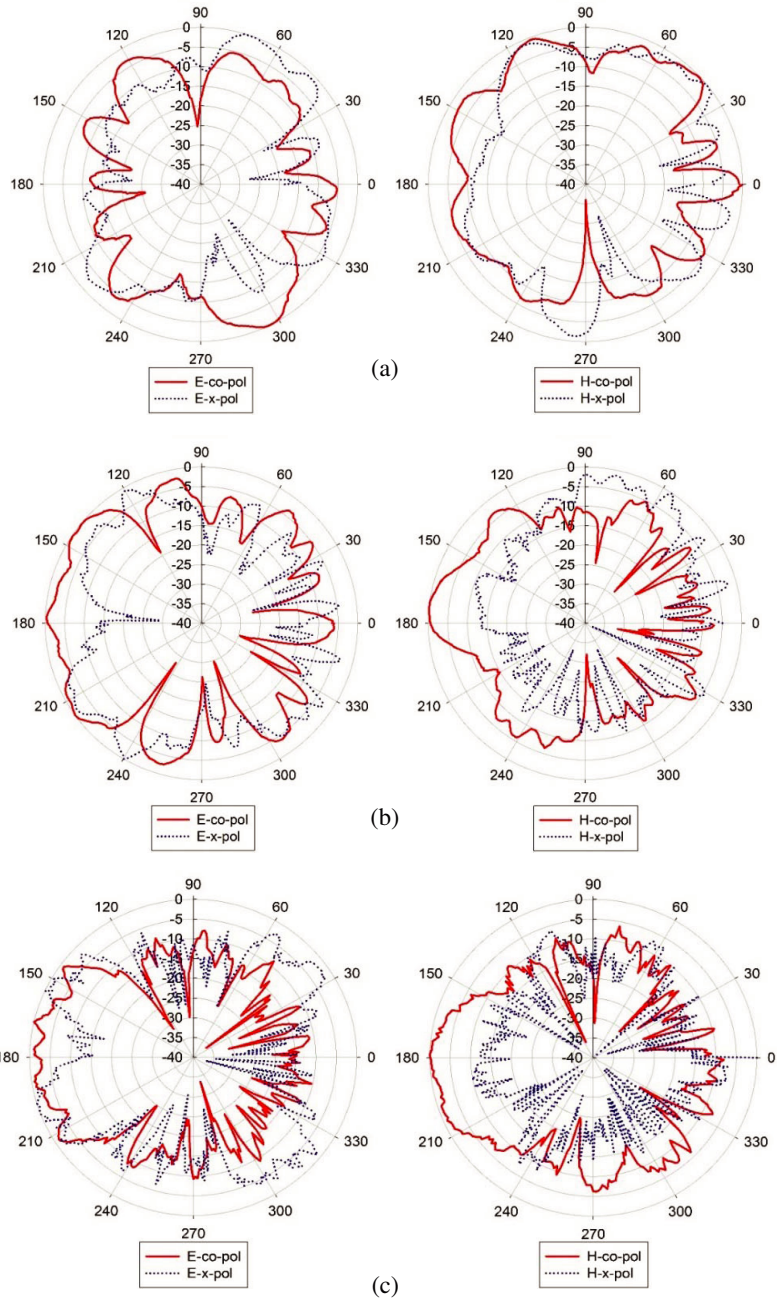

Figure 16. Measured radiation patterns at (a) 3.2 GHz, (b) 6.8 GHz and, (c) 9 GHz.

of the PIN diode switch BAP64-02 decreases at higher frequencies (more than 2 GHz) as investigated in [41].

Figure 15 shows the measured gain of the proposed filtering-antenna in case 1 using ideal switches. The results show that the gain of the proposed filtering-antenna is more than 1 dB with a peak value of 4.96 dB over the operating band from 2.5 to 10 GHz except that at the band notches frequencies, the gain significantly decreases. However, the gain is decreasing gradually over the operating band from 10 to 13.5 GHz due to the antenna misalignment and surrounding environment [42]. In addition, the dissipation factor of the substrate and the presence of higher order operational modes contribute to reducing the gain at higher frequencies [43–45].

Figure 16 illustrates the measured normalized radiation patterns of the proposed filtering-antenna

in case 1 using ideal switches. The measured radiation pattern including the co-polarization (co-pol) and cross-polarization (x-pol) in the H-plane and E-plane at several frequencies. It can be observed that the proposed filtering-antenna provides omnidirectional radiation patterns. However, the ripples problem occurs for all frequencies due to the small size of the patch and the reflections into the field between the antenna under test and reference antenna [42]. It is noted that the radiation patterns degrade at higher frequencies because of the presence of higher order operational modes. Also, it is noted that the cross-polarization of the radiation patterns degrades slightly with increasing frequency, which becomes slightly directional at higher frequencies. Therefore, the peak sidelobe level of the H-plane at 9 GHz does not exceed -5 dB.

6. CONCLUSION

A modified UWB monopole antenna integrated with simple and novel technique to achieve dual sharp band notches has been reported. By using microstrip transition between the feedline and the patch, and block with triangular shape slot loaded on both sides of the circular patch, the performance of the antenna is improved. The proposed design without resonant structures shows that wideband performance covers the entire UWB frequency band (3.1–10.6 GHz). Placing two DSRR above the ground plane of the antenna provides dual sharp band notches. The position of the created notch is tuned by varying the length of the DSRR. By employing a PIN diode switch in each DSRR, the frequency reconfiguration feature is achieved. The results show that the proposed filtering-antenna provides wide impedance bandwidth with reconfigurable dual band notches to filter out WiMAX and HiperLAN2 frequencies. Therefore, the proposed design is a good candidate for modern cognitive radio communications and UWB applications.

ACKNOWLEDGMENT

The authors gratefully acknowledge UTeM Zamalah Scheme, Universiti Teknikal Malaysia Melaka (UTeM) and Ministry of Higher Education for supporting this research work.

REFERENCES

1. Liao, X.-J., H.-C. Yang, N. Han, and Y. Li, "UWB antenna with single or dual band-notches for lower WLAN band and upper WLAN band," *Electron. Lett.*, Vol. 46, No. 24, 1593, 2010.
2. Jusoh, M. R. K. M., M. F. Jamlos, M. H. M. M. F. Malek, M. A. Romli, Z. A. Ahmad, and and M. S. Zulkifli, "A reconfigurable ultrawideband (UWB) compact tree-design antenna system," *Progress In Electromagnetics Research*, Vol. 30, 131–145, 2012.
3. Osman, M. A. R., M. K. a Rahim, N. a Samsuri, H. a M. Salim, and M. F. Ali, "Embroidered fully textile wearable antenna for medical monitoring applications," *Progress In Electromagnetics Research*, Vol. 117, 321–337, 2011.
4. Rahimi, M., R. A. Sadeghzadeh, and F. B. Zarrabi, "Band-notched UWB monopole antenna design with novel feed for taper rectangular radiating patch," *Progress In Electromagnetics Research C*, Vol. 47, 147–155, 2014.
5. Labade, R., S. Deosarkar, and N. Pisharoty, "Compact integrated bluetooth UWB antenna with quadruple bandnotched characteristics," *Int. J. Electr. Comput. Eng.*, Vol. 5, No. 6, 1433–1440, 2015.
6. Cal, G., P. Bari, and R. David, "Anew triple band circularly polarized square slot antenna design with crooked t and f-shape strips for wireless applications," *Progress In Electromagnetics Research*, Vol. 125, 503–526, 2012.
7. Liao, Z., F. Zhang, G. Xie, W. Zhai, and L. Chen, "An omni-directional and band-notched ultra wideband antenna on double substrates crossing," *Progress In Electromagnetics Research C*, Vol. 22, 231–240, 2011.
8. Chu, Q. X. and Y. Y. Yang, "A compact ultrawideband antenna with 3.4/5.5 GHz dual band-notched characteristics," *IEEE Trans. Antennas Propag.*, Vol. 56, No. 12, 3637–3644, 2008.

9. Morabito, A. F., A, R. Lagana, and T. Isernia, "Isophoric array antennas with a low number of control points: A 'Size Tapered' solution," *Progress In Electromagnetics Research Letter*, Vol. 36, 121–131, 2013.
10. Rocca, P. and A. F. Morabito, "Optimal synthesis of reconfigurable planar arrays with simplified architectures for monopulse radar applications," *IEEE Trans. Antennas Propag.*, 1–11, 2014.
11. Sam, W. Y. and Z. Zakaria, "A review on reconfigurable integrated filter and antenna," *Progress In Electromagnetics Research B*, Vol. 63, 263–273, 2015.
12. Haider, N., D. Caratelli, and A. G. Yarovoy, "Recent developments in reconfigurable and multiband antenna technology," *Int. J. Antennas Propag.*, 1–14, 2013.
13. Alhegazi, A., Z. Zakaria, N. A. Shairi, A. Salleh, and S. Ahmed, "Review of recent developments in filtering-antennas," *Int. J. Commun. Antenna Propag.*, Vol. 6, 125–131, 2016.
14. Yadav, A., D. Sethi, and R. K. Khanna, "Slot loaded UWB antenna: Dual band notched characteristics," *AEU — Int. J. Electron. Commun.*, Vol. 70, No. 3, 331–335, 2016.
15. Emadian, S. R. and J. Ahmadi-Shokouh, "Very small dual band-notched rectangular slot antenna with enhanced impedance bandwidth," *IEEE Trans. Antennas Propag.*, Vol. 63, No. 10, 4529–4534, 2015.
16. Mehranpour, M., J. Nourinia, C. Ghobadi, and M. Ojaroudi, "Dual band-notched square monopole antenna for ultrawideband applications," *IEEE Antennas Wirel. Propag. Lett.*, Vol. 11, 172–175, 2012.
17. Jiang, D., Y. Xu, R. Xu, and W. Lin, "Compact dual-band-notched UWB planar monopole antenna with modified CSRR," *Electron. Lett.*, Vol. 48, No. 20, 1250, 2012.
18. Gomes, C. and M. Z. A. Kadir, "Improved dual band-notched UWB slot antenna with controllable notched bandwidths," *Progress In Electromagnetics Research*, Vol. 113, 333–349, 2011.
19. Tang, Z., X. Wu, Z. Xi, and S. Hu, "Novel compact dual-band-notched ultra-wideband printed antenna with a parasitic circular ring strip," *Int. J. Microw. Wirel. Technol.*, 1–7, 2015.
20. Moosazadeh, M., A. M. Abbosh, and Z. Esmati, "Design of compact planar ultrawideband antenna with dual-notched bands using slotted square patch and pi-shaped conductor-backed plane," *IET Microwaves, Antennas Propag.*, Vol. 54, No. 9, 2053–2056, 2012.
21. Ojaroudi, M., N. Ojaroudi, and N. Ghadimi, "Dual band-notched small monopole antenna with novel W-shaped conductor backed-plane and novel T-shaped slot for UWB applications," *IET Microwaves, Antennas Propag.*, Vol. 12, 181–185, 2013.
22. Hu, Z., Y. Hu, Y. Luo, and W. Xin, "A novel rectangle tree fractal UWB antenna with dual band notch characteristics," *Progress In Electromagnetics Research C*, Vol. 68, 21–30, 2016.
23. Saxena, A. and R. P. S. Gangwar, "A compact UWB antenna with dual band-notched at WiMAX and WLAN for UWB applications," *2016 Int. Conf. Electr. Electron. Optim. Tech.*, 4381–4386, 2016.
24. Abdollahvand, M., G. Dadashzadeh, and D. Mostafa, "Compact dual band-notched printed monopole antenna for UWB application," *IEEE Antennas Wirel. Propag. Lett.*, Vol. 9, 1148–1151, 2010.
25. Lee, D. H., H.-Y. Yang, and Y.-K. Cho, "Ultra-wideband tapered slot antenna with dual band-notched characteristics," *IET Microwaves, Antennas Propag.*, Vol. 8, No. 1, 29–38, 2014.
26. Oraizi, H. and N. Valizade Shahmirzadi, "Frequency- and time-domain analysis of a novel UWB reconfigurable microstrip slot antenna with switchable notched bands," *IET Microwaves, Antennas Propag.*, Vol. 11, No. 8, 1127–1132, 2017.
27. Gao, G., B. Hu, L. He, S. Wang, and Y. Chen, "Investigation of a reconfigurable dual notched UWB antenna by conceptual circuit model and time-domain characteristics," *Microw. Opt. Technol. Lett.*, Vol. 59, No. 6, 1326–1332, 2017.
28. Kumar, A., I. B. Sharma, and M. M. Sharma, "Reconfigurable circular disc monopole UWB antenna with switchable two notched stop bands," *India Conf. (INDICON), 2016 IEEE Annu.*, 2–5, 2016.
29. Abunjaileh, A. I., "Multimode and multiband microstrip antennas," PhD Thesis, University of Leeds, 2007.

30. Tiang, J., M. Islam, N. Misran, and J. Mandeep, "Circular microstrip slot antenna for dual-frequency RFID application," *Progress In Electromagnetics Research*, Vol. 117, 425–434, 2011.
31. Pozar, D. M., *Microwave Engineering*, Vol. 1, 144–146, University Massachusetts Amherst, 2011.
32. Srifi, M. N., S. K. Podilchak, M. Essaaidi, and Y. M. M. Antar, "Compact disc monopole antennas for current and future ultrawideband (UWB) applications," *IEEE Trans. Antennas Propag.*, Vol. 59, No. 12, 4470–4480, 2011.
33. Alhegazi, A., Z. Zakaria, N. A. Shairi, A. Salleh, and S. Ahmed, "Integrated filtering antenna with high selectivity band rejection for UWB applications," *Przeglad Elektrotechniczny*, No. 9, 224–228, 2016.
34. Gheethan, A. A. and D. E. Anagnostou, "Dual band-reject UWB antenna with sharp rejection of narrow and closely-spaced bands," *IEEE Trans. Antennas Propag.*, Vol. 60, No. 4, 2071–2076, 2012.
35. Hamid, M. R., P. S. Hall, P. Gardner, and F. Ghanem, "Switched WLAN-wideband tapered slot antenna," *Electron. Lett.*, Vol. 46, No. 1, 23, 2010.
36. Rayno, J. T. and S. K. Sharma, "Frequency reconfigurable spirograph planar monopole antenna (SPMA)," *Proc. ISAP2012, Nagoya, Japan*, 1305–1308, 2012.
37. Kim, D., "A high performance IBC-Hub transceiver for intrabody communication system," *Microw. Opt. Technol. Lett.*, Vol. 54, No. 12, 2781–2784, 2012.
38. Horn, A. F., P. A. Lafrance, and J. W. Reynolds, "The influence of test method, conductor profile, and substrate anisotropy on the permittivity values required for accurate modeling of high frequency planar circuits," *Circuit World*, Vol. 38, No. 4, 219–231, 2012.
39. Nasrabadi, E. and P. Rezaei, "A novel design of reconfigurable monopole antenna with switchable triple band-rejection for UWB applications," *Int. J. Microw. Wirel. Technol.*, 1–7, 2015.
40. Semiconductors, N. X. P., "BAP64-02," *NXP Semiconductor Malaysia Sdn. Bhd.*, 2015, Available: http://www.nxp.com/documents/data_sheet/BAP64-02.pdf. [Accessed: 20-Dec.-2016].
41. Shairi, N. A., Z. Zakaria, A. M. S. Zobilah, B. H. Ahmad, and P. W. Wong, "Design of SPDT switch with transmission line stub resonator for WiMAX and LTE in 3.5 GHz band," *ARPN J. Eng. Appl. Sci.*, Vol. 11, No. 5, 3198–3202, 2016.
42. Rahman, T. A., "Reconfigurable ultra wideband antenna design and development for wireless communication," PhD, Universiti Teknologi Malaysia, 2008.
43. Tang, M.-C., R. W. Ziolkowski, and S. Xiao, "Compact hyper-band printed slot antenna with stable radiation properties," *IEEE Trans. Antennas Propag.*, Vol. 62, No. 6, 2962–2969, 2014.
44. Tang, M., S. Member, H. Wang, T. Deng, S. Member, and R. W. Ziolkowski, "Compact planar ultrawideband antennas with continuously tunable, independent band-notched filters," *IEEE Transactions on Antennas and Propagation*, Vol. 64, No. 8, 3292–3301, 2016.
45. Biomedica, I. and E. D. Telecomu, "Design of a novel super wide band circularhexagonal fractal antenna," *Progress In Electromagnetics Research*, Vol. 133, 53–89, 2013.